Influence of the synthesis parameter on the interlayer and framework structure of lamellar octadecyltrimethylamonium kanemite.

Juan I. Corredor[1], Agustín Cota[2], Esperanza Pavón[3], Francisco J. Osuna[4], María D. Alba[4,*]

[1] Unidad de RMN-SCAI. Campus de Rabanales. Edificio Ramón y Cajal. Universidad de Córdoba, 14071-Córdoba (SPAIN)

[2] Laboratorio de Rayos-X. CITIUS. Universidad de Sevilla. Avda. Reina Mercedes, 4b. 41012-Sevilla (SPAIN)

[3] Unité de Catalyse et de Chimie du Solide, UCCS, CNRS, UMR8181, Université Lille Nord de France, 59655 Villeneuve d'Ascq (FRANCE)

[4] Instituto Ciencia de los Materiales de Sevilla. Consejo Superior de Investigaciones Científicas-Universidad de Sevilla, Avda. Americo Vespucio, 49, 41092 Seville (SPAIN)

ABSTRACT

Inorganic-organic nanostructures, used as host materials for selective adsorption of functional molecules and as mesostructured materials precursors, can be constructed by the interlayer modification of inorganic layered materials with surfactants. The formation mechanism is mainly determined by the surfactant assemblies in the 2D limited space. In this paper, a detailed structural analysis of the lamellar mesophases prepared from kanemite, a lamellar silicate, and octadecyltrimethylammonium (ODTMA) under various

* Corresponding author. Tel.: +34 954489546
E-mail address: alba@icmse.csic.es (M.D. Alba).

conditions was reported. The adsorbed amount of ODTMA and the long and short range structural order were explored by TGA, XRD, IR/FT and MAS NMR spectroscopies. The results revealed that ODMTA molecules were efficiently intercalated in the interlayer space of kanemite and, in all synthesis conditions, an ordered lamellar structure was obtained. The ODTMA adsorption in kanemite not only caused changes in the interlayer space but also in the silicate framework, where five-member rings were formed. The characteristics of the final products were influenced by the synthesis conditions, although the separation mode, filtration or centrifugation, was not relevant. Therefore, the adsorption conditions of ODTMA in kanemite will contribute to the design of novel layered materials with potential environmental and technological use.

Keywords. Lamellar silicates, Octadecyltrimethylamonium, kanemite, mesostructure.

Graphical abstract.

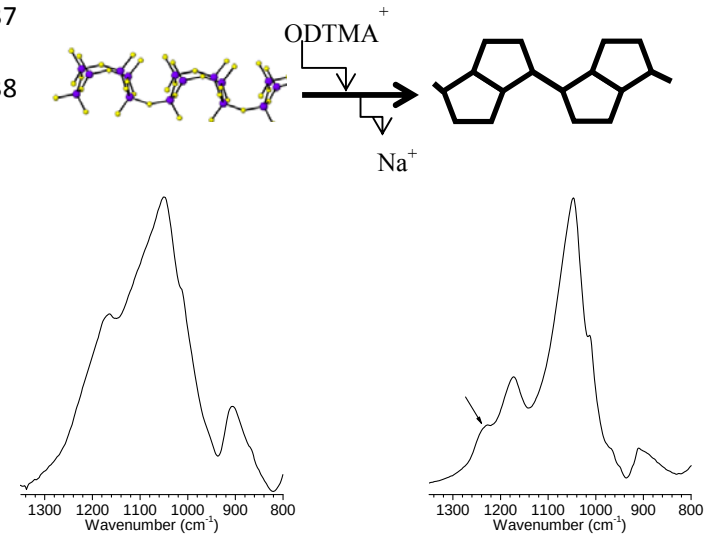

1. Introduction

The interlayer modification of inorganic layered materials with surfactants was used to construct inorganic-organic nanostructures that were used as host materials for further intercalation and selective adsorption of functional molecules (Ogawa et Kuroda, 1995, 1997). In the wide variety of inorganic layered materials, the layered polysilicates such as magadiite, octosilicate, and kanemite were unique because their frameworks are composed of only tetrahedral SiO_4 units and both hydrated alkali metal ions and silanol (Si-OH) groups are present in the interlayer region (Lagaly, 1979). Among them, kanemite received much attention due to its high capacity of development of ordered mesoporous silicas. Yanagisawa et al.(1990) were the first that described the formation of mesoporous silica derived from kanemite. Later, Inagaki et al. (1993, 1996) reported the synthesis of hexagonal mesoporous silicas (designated as FSM-16) from kanemite intercalated with hexadecyltrimethylamonium (HDTMA).

During the synthesis, a kanemite-surfactant mesophase was formed as precursor and the environment of tetrahedral SiO_4 units in kanemite sheets were transformed in a three-dimensional (3-D) silicate network, SiO_4 species with both $Q^3$and Q^4 environments being detected (Inagaki et al., 1993; Yanagisawa et al., 1990). The presence of this layered intermediate determined the final mesoporous silica structure (lamellar, hexagonal or cubic); however, this intermediate has not been studied in deep. It is well-known that the formation mechanism of the final mesoporous silica was determined by the surfactant assemblies in the 2D limited space in addition to the structural changes of the silicate sheets. Kimura and Kuroda (2009) observed that: i) Layered surfactant–silicate compounds were formed using surfactants that tended to be assembled as lamellar phases. Even after an

64 acid treatment, the produced surfactant silicates were not transformed into other phases. ii)
65 2D hexagonal phases were formed through the creation of layered compounds and the
66 fragmentation of silicate sheets when surfactants that tended to be assembled as lamellar
67 and rod-like phase were used. iii) 2D orthorhombic phases were formed by mild acid
68 treatment of layered complexes retaining the silicate frameworks of kanemite. iv)
69 Disordered phases were formed using surfactants with a tendency to assemble spherically
70 because the silicate sheets were hard to completely bend along the spherical assemblies.
71 The bending of the silicate sheets of kanemite occurred during the reactions with the
72 surfactants. However, the silicate sheets were not able to bend freely and the final phase
73 depended on the nature of the silicate sheet and the HDTMA/Si molar ratio (Tamura et al.,
74 2007).

75 Layered silicates, clay minerals, intercalated with alkyltrimethylamonium (C_nTMA)
76 had, as well, useful applications for the removal of oil, toxic chemicals and humic materials
77 from water (Yariv, 1996; Zhao and Vance, 1998), as adsorbents for organic pollutants
78 (Taylor, 1992), rheological control agents (Sutton, 2000) and reinforcing fillers for plastics
79 and electric materials (Pinnavaia et al., 1996; Sand et al., 2003). Those applications were
80 possible thanks to the change from hydrophilic to hydrophobic properties, which was
81 proved to be enhanced when alkyl chain length of C_nTMA increases (Pazos et al., 2012).

82 Kimura et al. (2000) investigated the synthesis and characterization of layered
83 HDTMA–silicate compounds in detail and observed that regardless of the reaction
84 temperature layered HDTMA-silicate were obtained as pure phase but they showed
85 structural changes in the silicate framework. Nevertheless, the influence of surfactant chain
86 length and, therefore, the packing degree of octadecyltrimethylamonium (ODTMA) in the

kanemite interlayer was not explored, despite their importance in the ecological properties of the final compound.

In this paper, we report a detailed structural analysis of the lamellar ODTMA mesophases prepared from kanemite and octadecyltrimethylammonium (ODTMA) under various conditions such as washing and separation process, pH adjustment, ODTMA/Si molar ratio, stirring temperature and time.

2. Experimental Section

2.1. Preparation of kanemite.

Na-kanemite was prepared by dissolution of appropriate amounts of sodium chloride (Si/Na=1) in 50 g of a sodium silicate solution (ALDRICH, 12.6 % Si, 13.8 % NaOH). The reaction mixture was heated at 100 °C for 72 h in an open crucible and the resulting product calcined at 700 °C for 6 h. After cooling to room temperature, the solid was dispersed in 20 times its weight of water and stirred for 15 minutes. The silicate was recovered by filtration, washed with distilled water (solution/solid=10 wt%), and, then dried in air at room temperature (Alba et al., 2006).

2.2. Reactions of kanemite with ODTMA Surfactant.

A 1g amount of Na-kanemite was added to 20, 100 or 200 mL of an aqueous solution of 0.1 M octadecyltrimethylammonium bromide ($C_{18}H_{37}(CH_3)_3NBr$, ODTMABr, Sigma-Aldrich), where ODTMA/Si molar ratios were 0.2, 1.0, and 2.0, respectively. The

111 samples were stirred at 70 ºC for 3 days. Then, the products were washed with an
112 ethanol/water (1:1 v/v) mixture, filtered and air dried.

113 To examine the effect of the reaction temperature and time, 1 g of Na-kanemite was
114 dispersed in 20 mL of an aqueous solution of 0.1 M ODTMABr and stirred at 70 ºC or 90
115 ºC for 2, 3 and 7 days. The products were washed with an ethanol/water (1:1 v/v) mixture,
116 filtered and air dried.

117 The effect of pH was examined for the ODTMA/Si molar ratio of 0.2 comparing the
118 synthesis at the dispersion pH value of 12.08 and at the pH valued adjusted at 8.0 with HCl
119 or HF 0.1 N. After the dispersion stirring at 90 ºC for 3 days, the products were washed
120 with an ethanol/water (1:1 v/v) mixture, filtered and air dried.

121 Finally, to examine the effect of the surfactant removal efficiency, 1 g of Na-
122 kanemite was dispersed in 20 mL of an aqueous solution of 0.1 M ODTMABr and stirred at
123 70 ºC for 3 days. The products were washed with an ethanol/water (1:1 v/v) mixture,
124 filtered or centrifuged and air dried. In parallel, the excess of surfactant was removed by
125 filtration or centrifugation, without washing, and air dried.

126 The name of the products and the synthesis conditions were summarized in Table 1.

127

128 *2.3. Characterization.*

129

130 Thermogravimetric (TG) analyses were performed using a TA (SDT-Q600)
131 instrument to determine the amount of residual water and surfactant in the Textural and
132 Thermal Analysis Service of the ICMS (CSIC-US, Seville, Spain). The sample temperature
133 was increased up to 550 °C at a rate of 10 °C·min^{-1} in air and it was maintained during 3
134 hours.

Powder X-ray diffraction (XRD) patterns, in the region from 1° to 12° 2θ, were obtained by using a transmission X-ray diffractometer Panalitical X´Pert Pro. equipped with a Cu Kα radiation source in the X-ray Diffraction Service of the ICMS (CSIC-US, Seville, Spain). Diffractograms were obtained with a step size of 0.01° 2θ and a time step of 3.0 s. Difraction peaks were analysed using the DIFFRAC^{plus} Evaluation package.[†]

Infrared spectra (FT/IR) were recorded in the range 4000–400 cm^{-1} by the Spectroscopy Service of the ICMS (CSIC-US, Seville, Spain), as KBr pellets, using a Nicolet spectrometer (model 510P) with a nominal resolution of 4 cm^{-1}.

Single-pulse (SP) MAS-NMR spectra were recorded at the Spectroscopy Service of SCAI (University of Cordoba, Spain) using a Bruker AVANCE WB400 spectrometer equipped with a multinuclear probe. Powdered samples were packed in 4 mm zirconia rotors and spun at 12 kHz. ^{1}H MAS spectra were obtained using typical π/2 pulse widths of 4.25 μs and a pulse space of 5 s. ^{29}Si MAS NMR spectra were acquired at a frequency of 79.49 MHz, using a pulse width of 1.4 μs (π/2 pulse length = 4.2 μs) and a delay time of 300 s. ^{13}C MAS NMR spectra were acquired with proton decoupling at a frequency of 100.62 MHz, using a pulse width of 1.5 μs (π/2 pulse length = 4.5 μs) and a delay time of 2 s. ^{23}Na MAS NMR spectra were acquired at a frequency of 105.84 MHz, using a pulse width of 1.1 μs (π/2 pulse length = 6.6 μs) and a delay time of 0.1 s. The chemical shift values were reported in ppm with respect to tetramethylsilane for ^{1}H, ^{29}Si and ^{13}C and from a 0.1 M NaCl solution for ^{23}Na. Spectra were simulated using the DMFIT software (Massiot et al., 2002) assuming infinite spinning speed. A Gaussian-Lorentzian model was

[†] © 2010 Bruker AXS GmbH, Karlsruhe, Germany

used for all the peaks, and fitted parameters were: amplitude, position, linewidth and Gaussian-Lorenztian ratios.

3. Results and Discussion

3.1. ODTMA adsorption and hydrophobicity of the interlayer space.

The TG curves of Na-kanemite (not shown) showed a four-step dehydration process: step A up to 105 °C, step B from 105 to 159 °C, step C from 159 to 216 °C and step D from 216 to 325 °C (Corredor et al., 2013). Beneke and Lagaly (Beneke et al., 1997) suggested the presence of two types of water in the interlayer space of kanemite, with one type forming an interlamellar monolayer of water molecules and the other being trapped within vacancies of the folded SiO_3OH hexagonal rings. Additional water molecules were adsorbed on the external surface, with hydroxyl groups being the source of the evolved water. Each step in the TG curve could not be assigned exclusively to one particular species. Thus, the surface water and interlamellar water were released in step A, water within the hexagonal rings may be released in steps B and C and some of the hydroxyl groups were released in step D (Hayashi, 1997). The weight loss was calculate in two regions: 25–200 °C due to water loss and 200-550 ºC due to hydroxyl groups (Table 1) and both weight loss were close to the ideal composition of Na-kanemite (Kuroda, 1996).

To investigate the structure and properties of the alkyltrimethylammonium molecules adsorbed onto organokanemite, it was necessary to evaluate the amount of adsorbed surfactant and it was monitored by TGA (Osman et al., 2000; Osman and Suter, 2002; Osman et al., 2003). Two endothermic and two exothermic changes were seen in the DTA

curve of the organokanemites (not shown). The endothermic changes, between 25–200 °C, were due to water loss and the exothermic changes, between 200-500 ºC, were due to the decomposition of the ODTMA (Önal and Sarikaya, 2008). Therefore, the TG analysis was divided into two parts. First, the amount of interlayer water was determined from the weight loss in the temperature range of 25–200 °C. The weight loss between 200 and 550 °C was then used, with the assumption that in the as-made kanemite some of the hydroxyl groups were released in this range, to determine the number of ODTMA molecules adsorbed by the kanemite (Xie et al., 2001).

In general, the amount of adsorbed ODTMA of the ODTMA-K-1, ODTMA-K-2, ODTMA-K-3 and ODTMA-K-4 (Table 1) ranged between 17.65 % w/w and 34.22 % w/w which were lower than the theoretical value for a total adsorption, 42.54 % w/w. The ODTMA amount diminished up to the half after washing but the separation process (filtration or centrifugation) didn´t seem to have a significant influence. The ^{23}Na MAS NMR spectra (Fig. SI1a) evidenced the decrease of the Na NMR signal when samples were not washed, in good agreement with a higher amount of ODTMA exchanged. The replacement of the hydrated Na^+ by an organic cation changed the surface properties from hydrophilic to hydrophobic (Jayne and Boyd, 1991), which cause a reduction of the water content proportional to the amount of adsorbed ODTMA. The amount of the ODTMA in the starting mixture would allow replacing only 36 % of the Na^+, explaining the presence of water molecules in the products.

The comparison of the TG of the ODTMA-K-1, ODTMA-K-5, ODTMA-K-6, ODTMA-K-7, ODTMA-K-8 and ODTMA-K-9 (Table 1) allowed evaluating the effect of temperature and time of stirring in the adsorption of ODTMA. The amount of adsorbed ODTMA ranged between 17.34 % w/w and 31.22 % w/w which were lower than the

theoretical value for a total adsorption, 42.54 % w/w. At each reaction time, the amount of adsorbed ODTMA increased with temperature -at 2 days of stirring, the weight loss in this region was almost double at 90 ºC than at 70 ºC-, but the influence of temperature decreased at longer stirring time - at 7 days, the weight loss was almost the same at both temperatures-. ^{23}Na MAS NMR spectra (Fig. SI1b) showed that despite the adsorbed amount of ODTMA, the intensity of ^{23}Na NMR signal decreases when the temperature increases. Hydrolysis processes in the interlayer space, favored with increasing temperature and time, could be the accountable of this behavior.

A direct relation between ODTMA adsorption and water loss was not observed, thus, the hydrophobicity of organokanemite could be related not only to the substitution of Na^+ by ODTMA but also to the ODTMA packaging. At reaction time above 2 days, the weight loss due to water removal was higher at 70 ºC than at 90 ºC and the minimum water content and the minimum intensity of the ^{23}Na NMR signal (higher hydrophobic character of interlayer space) was reached when the synthesis conditions were 90 ºC and 7 days.

The analysis of the pH effects on the adsorbed surfactant and the hydrophobic character of the organokanemite were made by the comparison of the TG of the ODTMA-K-8, ODTMA-K-10 and ODTMA-K-11 (Table 1). The amount of adsorbed ODTMA ranged between 21.98 % w/w and 36.69 % w/w which were lower than the theoretical value for a total adsorption, 42.54 % w/w. However, the pH correction favored the adsorption of ODTMA which was higher when the adsorption was carried out in a HCl media than in a HF media. The weight loss due to water removal, 25-200 ºC, diminished proportionally to the amount of the adsorbed ODTMA due to an increment of the hydrophobicity. The ^{23}Na MAS NMR spectra (Fig. SI1c) showed that the pH adjustment provoked almost the

disappearance of the ^{23}Na NMR signal, as a consequence of the high ODTMA adsorption and the released of protons by the acid media.

The analysis of the effect of the ODTMA/Si molar ratio on the adsorbed surfactant and the hydrophobic character of the organokanemite were made by the comparison of the TG of the ODTMA-K-1, ODTMA-K-12 and ODTMA-K-13 (Table 1). As the ODTMA/Si ratio increased in the starting mixture, the amount of adsorbed ODTMA increased up to 43.18 % w/w but the total substitution of Na^+ by ODTMA was not achieved, as it could be seen on the ^{23}Na MAS NMR spectra (Fig. SI1d), even when its amount in the synthesis composition was enough. The weight loss due to water removal, between 25-200 ºC, and the intensity of ^{23}Na NMR signal diminished proportionally to the amount of the adsorbed ODTMA, explained by an increment of the hydrophobicity when the ODTMA amount in the synthesis mixture increased.

As previously reported (Corredor et al., 2013), the ^{1}H MAS NMR spectra of Na-kanemite (Fig. SI2a) showed two types of signals at around 15.5 and 5.3 ppm (signals I and II, respectively), which were assigned to hydroxyl groups involved in hydrogen bonds and water molecules, respectively (Hayashi, 1997). In general, the ^{1}H MAS NMR spectra of organokanemite (Fig. S21) exhibited the total disappearance of the signal at ca. 15.5 ppm due to the brokenness of the hydrogen bonds between layers as a consequence of the intercalation of ODTMA and a drastically diminishing of the water signal at ca. 5.3 ppm, in good agreement with the TG data which showed an increase of the interlayer space hydrophobicity. Additionally, two new set of signal were observed in those spectra. A broad signal at ca. 1.5 ppm (signal IV) is due to isolated silanol protons (Yesinowski et al., 1988) and agreed with the brokenness of the OH involved in the hydrogen bonding. And the three narrow signals in the range between 0 and 3.5 ppm are due to the ODTMA, where

the two signals at 1.3 and 0.9 ppm (signals V and VI) are due to the alkyl chain (Alba et al., 2011) and the signal at 3.2 ppm (signal III) is due to the methyl groups of the head (Abraham and Mobli, 2008).

The comparison of the ^{1}H MAS NMR spectra of ODTMA-K-3 vs ODTMA-K-1 and ODTMA-K-4 vs ODTMA-K-2 (Fig. SI2a) showed the absence of the signal at ca. 1.5 ppm (signal IV, isolated OH groups) in the no-washing samples. This inferred that the excess of the ODTMA in those samples (ODTMA-K-3 and ODTMA-K-4) was adsorbed on specific sites (isolated OH groups) and not in the interlayer space of kanemite (no specific sites).

The analysis of TG as a function of temperature and time of stirring showed that there was not a direct relation between ODTMA adsorption and water loss and it was confirmed by the intensity of water signal (at ca. 5.3 ppm, signal II) in the ^{1}H MAS NMR spectra (Fig. SI2b). However, these spectra revealed a parallel intensity increment of the signal at ca. 5.3 ppm, water, and the signal at ca. 1.5 ppm, isolated OH groups, at higher stirring temperature which could explain the higher water loss (probably due to water adsorbed on surface among than those in the Na^{+} coordination sphere) in spite of the higher adsorbed ODTMA observed by the TG data. As observed by TG, after 7 days of stirring, both temperatures caused the same effect.

3.2. Package structure of the ODTMA in the interlayer space.

The XRD patterns of the organokanemites were shown in the left side of Fig. 1-4 and all of them showed two reflections between 2 and 3º 2θ and 4 and 5º 2θ which corresponded to the *001* and *002* planes, and proved the layered nature of the products. In addition, in all XRD patterns, except in ODTMA-K-10 and ODTMA-K-11, a reflection at

8.65º 2θ, *020* reflection of Na-kanemite (Corredor et al., 2013), was observed. It agreed with the fact that the amount of ODTMA employed was not enough for the total replacement of Na^+, as deduced from the TG data (Table 1). In the case of the ODTMA-K-10 and ODTMA-K-11 (Fig. 3, left), the absence of Na-kanemite *020* reflection could be interpreted by its solubilization in HCl or HF medium or the Na^+ exchange by proton. The last interpretation should be ruled out because acid protons were no detected by ^1H MAS NMR (see Fig. SI1c).

Although the basal spacings of *n*-alkylammonium intercalated compounds generally tend to be larger with the increase in the contents of organic fractions (Weiss, 1963), this tendency was not found for the lamellar ODTMA silicates derived from kanemite, as previously observed in HDTMA-kanemite (Kimura et al., 2000). It could be interpreted on the basis of ^1H MAS NMR spectra (Fig. SI1) that showed ODTMA adsorption not only occurred at no specific sites (cationic exchange) but also at specific ones (associated to isolated OH groups).

The washing process did not affect the long range order of organokanemite (Fig. 1, left) and the only effect was an increase of the intensity of the Na-kanemite *020* reflection after washing as consequence of the partial removal of ODTMA, as observed by TGA. Additionally, the XRD of ODTMA-K-3, which exhibited the higher ODTMA weigh loss by TGA, showed a small reflection at 3.07º 2θ corresponding with free ODTMABr.

The effect of the stirring time and temperature on the long range order of the organokanemite could be analyzed from the relative intensity of the *002* reflection *vs 001* reflection (Fig. 2, left). As temperature and time increased, the intensity of *002* reflection increased with the exception of 7 days, when both temperatures gave rise the same results. Thus, 90 ºC and 3 days of stirring gave the best ordered lamellar structure except in the

299 case of pH adjustment, from 12.1 to 8.0, with HCl or HF (Fig. 3, left). Organokanemites
300 synthesized in the HCl or HF media showed lamellar structure with a d_{001}=4.02-4.04 nm
301 but the *002* reflections were absents.

302 The ODTMA/Si ratio in the synthesis mixture did not affect the long ranger order of the
303 organokanemite (Fig. 4, left) and the only effect was a drastically diminishing of the Na-
304 kanemite *020* reflection at high ODTMA/Si ratio. Even in the case of an excess of
305 ODTMA, ODTMA-K-12 and ODTMA-K-13, the reflection at 3.07º 2θ, due to free
306 ODTMABr, was not observed and it was in good agreement with the TG data (Table 1) that
307 revealed lowest ODTMA adsorption than cationic exchange capacity.

308 In no case was observed a XRD pattern due to a hexagonal phase as occurred with
309 HDTMA-kanemite (Kimura et al., 2000).

310 ^{13}C NMR MAS spectroscopy (Fig. 1-4, right) was used to probe the structure,
311 conformation and dynamics of the alkyl chains and gave an insight into the conformational
312 heterogeneity and differences in chain packing at the interfaces. In general, the ^{13}C NMR
313 spectra (Fig. 1-4, right) showed a set of signals that could be assigned as follows (Wang et
314 al., 1996): the terminal methyl group (C_{18}) of the alkyl chains appeared at around δ = 14.7
315 ppm, whereas the $C_{3,17}$ and C_2 carbons appeared at around δ = 23.5 ppm and 27.1 ppm,
316 respectively. The weak and broad peak at 67.0 ppm was assigned to the *N*-methylene group
317 (C_1) while the 54.1 ppm peak was associated with the *N*-methyl group (C_N). The remainder
318 of the internal methylenes (C_4-C_{16}) was lumped together in a doublet centered at 33.1 and
319 30.8 ppm.

320 A detailed analysis of the ^{13}C resonances of the internal methylenes (C_4-C_{16}) provided
321 information regarding the molecular conformation and packing. The peak at around $\delta \approx 33$
322 ppm was due to an all-*trans* conformation and the peak at lower frequency ($\delta \approx 30$ ppm)

was due to a dynamic average between the *gauche* and *trans* conformations (Wang et al., 2000). The contribution of each configuration depended on the synthesis parameters. The ratio between them was displayed in the figure as well.

The removal of up to the half amount of ODTMA after washing provoked a considerable increases in the *gauche* -*trans* conformation due to the lower packing degree of ODTMA in the interlayer space (Fig. 1, right) (Alba et al., 2011; Pazos et al., 2012). Same effect was observed when the ODTMA/Si was modified in the synthesis mixture (Fig. 4, right). The all-*trans* conformation was favored by filtering separation.

The observed high long-range order as consequence of the stirring time and temperature was also reflected in the increasing of the all-*trans* conformation of the ODTMA in the interlayer space (Fig. 2, right). The higher proportion of all-*trans* conformation was obtained at a stirring condition of 90 ºC for 3 days.

As it can be predicted the adjustment of pH with HCl or HF provoked a disordered lamellar structure where the most of ODTMA adopted a dynamic average between the *gauche* and *trans* conformations (Fig. 3, right).

3.3. Structural study of the organokanemite framework.

Whereas the ^{29}Si MAS NMR spectra of Na-kanemite showed a unique signal at -97.3 ppm due to Q^3 environment (Corredor et al., 2013), the ODTMA-kanemites showed the presence of SiO_4 species of both Q^3, signals in the range -95 to -101 ppm, and Q^4 environments, signals in the range -101 and -111 ppm, (Fig. 5-8, right) (Lippman et al., 1980). This NMR profile was observed in many cases as an evidence of the formation of a 3-D silicate network of the hexagonal structure (Inagaki et al., 1993); however, here the Q^4

347 silicate species were detected in the lamellar structure. This structural change of the silicate
348 frameworks was never found for organoammonium intercalation compounds of other
349 layered silicates (Ogawa and Kuroda, 1995), the Q^4 silicate species being related to the
350 unique structure of kanemite and was previously reported for HDTMA-kanemite (Kimura
351 et al., 2000). Those Q^4 environments were formed by the interlayer condensation, favored
352 by the structure of the kanemite. In fact, the individual silicate sheets of kanemite,
353 composed of SiO_4 tetrahedra, were wrinkled regularly and the adjacent Si-OH groups were
354 alternatively confronting each other, provoking the condensation of the interlayer (Gies et
355 al., 1998; Garvie et al., 1999; Vortmann et al., 1999). The loss of H···O···H bridges
356 between layer (see ^{1}H MAS NMR results) that accompanied the appearance of the Q^4
357 environments strengthened this idea.

358 The quantification of the ^{29}Si MAS NMR spectra was carried out from the
359 deconvolution of the spectra and the $Q^4/(Q^3+Q^4)$ ratios were summarized in Table 1. In
360 general, no relation between $Q^4/(Q^3+Q^4)$ ratio and adsorbed ODTMA was observed as
361 noted in the case of HDTMA-kanemite (Kimura et al., 2000). Only in the case of an
362 increment of ODTMA/Si ratio in the synthesis mixture (Fig. 8, left), the increment of
363 adsorbed ODTMA (see TG results) provoked an increment of $Q^4/(Q^3+Q^4)$ ratio from 0.27
364 to 0.52.

365 The peak intensity due to Q^4 silicate species increased and the Q^3 peaks were broadened
366 (Fig. 6, left) with the increase in the stirring temperature and time. The flexibility of the
367 silicate framework in kanemite became lower by intralayer condensation, and the lamellar
368 phases occurred more easily.

Although, the pH value intensely affected the behavior of silicate species in the reaction mixtures (Liebau, 1985), the adjustment of pH with HCl or HF did not affected the Q^4 formation as much as stirring temperature and time did (Fig. 7, left).

Vibrational spectroscopy could also provide valuable structural information which is complementary to that obtained from XRD and NMR and provided invaluable information regarding the hydrogen bonding, Si-O-Si bond angles, the network connectivity, and the size of the ring systems formed by SiO_4 tetrahedra in kanemite (Huang et al., 1998). Here, the bands in the 800 to 1300 cm^{-1} region were analyzed because they were attributed to SiO-stretching vibrations (Xi et al., 2005). Na-kanemite (Fig. SI3, left) exhibited IR bands at 1165, 1049 and 906 cm^{-1}. The high frequency band at about 1170 cm^{-1} was assigned to the asymmetric stretching vibrations of Si-O-Si bridges, ν_{as}(Si-O-Si), with angles close to 180° (Huang et al., 1999). The band at 1049 cm^{-1} was assigned to the stretching vibration of terminal $Si\text{-}O^-$ bonds, $\nu(Si\text{-}O^-)$, of the Q^3 species and the low frequency band at 906 cm^{-1} was due to the symmetric stretching vibrations of Si-O-Si bridges, ν_s(Si-O-Si) (Huang et al., 1998).

After ODTMA adsorption (Fig. 5-8, right), two small bands were observed at ca. 965 cm^{-1}, marked with asterisk in the Figures, due to vibrational mode of ODTMA molecules (see Fig. SI3, right). The intensity of these bands diminished after washing (Fig. 5, right) and increased with the initial ODTMA amount (Fig. 8, right), stirring time and temperature (Fig. 6, right) and after pH adjustment (Fig. 7, right). In these samples where the intensity of ODTMA vibrational bands were strong, the $\nu(Si\text{-}O^-)$ bands shifted to higher wavenumber which denoted an interaction between the ODTMA and the kanemite siloxane

layer immediately upon contact, as previously observed in montmorillonite intercalated with ODTMA (Xi et al., 2005).

A new vibrational band close to 1230 cm^{-1}, marked with + in Fig. 5-8 right, was observed in ODTMA-kanemites, as previously observed in magadiite and kenyite, and was attributed to the existence of five-membered rings (Garcés et al., 1988). The appearance of this band was accompanied of an intensity diminishing of the ν_{as}(Si-O-Si) vibrational band with angles close to 180°. The evidence of five-membered rings formation in ODTMA-kanemite could explain the existence of the Q^4 environment observed by ^{29}Si MAS NMR. The intensity of this vibrational band diminished after washing (Fig. 5, right) and increased with initial ODTMA amount (Fig. 8, right), stirring time and temperature (Fig. 6, right) and after pH adjustment (Fig. 7, right).

Finally, the IR/FT spectra of ODTMA-K-10 and ODTMA-K-11 (Fig. 7, right) were characterized by the absence of the ν_{as}(Si-O-Si) and ν_{s}(Si-O-Si) vibrational bands of kanemite which could be interpreted as the kanemite solubilization in the HCl or HF medium, as previously evidenced by XRD (Fig. 3, left).

4. Conclusions

ODMTA molecules were efficiently intercalated in the interlayer space of kanemite and an ordered lamellar structure was obtained in all synthesis conditions. The adsorbed ODTMA adopted a combination of all-*trans* and *trans-gauche* conformations.

The ODTMA adsorption in kanemite did not only caused a decrease in the water content of the interlayer space (hydrophobicity enhancement) but also produced changes in the silicate framework, which were found to be drastic when the adsorption was carried out

415 in HCl or HF medium. The main silicate framework change was the disruption of the
416 intralayer H···O···H bridges accompanied by the formation of SiO_4 Q^4 environments and
417 five-member rings.

418 The adsorbed amount of ODTMA and its decreased interlayer water content
419 (hydrophobicity), the long range order of organokanemite, the surfactant packing in the
420 interlayer and the reorganization of the silicate framework were highly affected by the
421 ODTMA/Si ratio, stirring temperature and time, pH adjustment and washing. However, the
422 influence of separation mode, filtration or centrifugation, was not relevant.

423 Those findings widen the understanding of the reaction system of kanemite with
424 ODTMA, and hence, contribute to the design of novel materials with useful potential
425 applications. On one hand, ODTMA-kanemites can be used for the preparation of layered
426 materials with tuned capacity for adsorption of organic-inorganic contaminants, due to the
427 partial hydrophobicity of the interlayer space. On the other, they can work as a precursor
428 for the design of new mesostructured silicates, due to the flexibility of the layer that keep
429 on after the adsorption, as evidenced by the persistence of Q^3 environment.

430

431 **Acknowledgement**

432

433 We would like to thank the DGICYT (project no. CTQ 2010-14874) and FEDER
434 for their financial supports.

435

436 **References**

437

438 Abraham, R., Mobli, M. (Eds.), 2011. Modeling ^{1}H NMR spectra of organic compounds:
439 Theory, applications and NMR prediction software. John Wiley Sons. ltd.
440 Alba, M.D., Castro, M.A., Orta, M.M., Pavón, E., Pazos, M.C., Valencia Rios, J.S., 2011.
441 Formation of organo-highly charged mica. Langmuir 27, 9711-9718.
442 Alba, M.D., Chain, P., Pavon, E., 2006. Synthesis and characterization of gallium
443 containing kanemite. Microporous Mesoporous Materials 94, 66-73.
444 Beneke, K., Lagaly, G., 1997. Kanemite - inner-crystalline reactivity and relations to other
445 sodium silicates. American Mineralogist 62, 763-771.
446 Corredor, J.I., Cota A., Pavón, E., Alba, M.D., 2013. Synthesis and characterization of
447 kanemite from fluoride-containing media: Influence of the akali cation. American
448 Mineralogist 98, 1000-1007.
449 Garcés, J. M., Rocke, S. C., Crowder, C. E., Hasha, D. L., 1988. Hypothetical structures of
450 magadiite and sodium octosilicate and structural relationships between the layered
451 alkali-metal silicates and the moderite-group and pentasil-group zeolites. Clays and
452 Clay Minerals 36, 409-418.
453 Garvie, L. A. J., Devouard, B., Groy, T. L., Camara, F., Buseck, P. R., 1999. Crystal
454 structure of kanemite, $NaHSi_2O_5$ center dot 3H(2)O, from the Aris phonolite, Namibia.
455 American Mineralogist 84, 1170-1175.
456 Gies, H., Marler, B., Vortmann, S., Oberhagemann, U., Bayat, P., Krink, K., Rius, J., Wolf,
457 I., Fyfe, C., 1998. New structures-new insights: Progress in structure analysis of
458 nanoporous materials. Microporous Mesoporous Materials 21, 183-197.
459 Hayashi, S., 1997. Solid-state NMR study of locations and dynamics of interlayer cations
460 and water in kanemite. Journal of Material Chemistry 7, 1043-1048.

461 Huang, Y., Jiang, Z., Schwieger, W., 1998. A vibrational study of Kanemite. Microporous
462 Mesoporous Materials 26, 215-219.
463 Huang, Y., Jiang, Z., Schwieger, W., 1999. Vibrational spectroscopic studied of layered
464 silicates. Chemistry of Materials 11, 1210-1217.
465 Inagaki, S., Fukushima, Y., Kuroda, K., 1993. Synthesis of highly ordered mesoporous
466 materials from a layered polysilicate. Journal of Chemical Society, Chemical
467 Communication 680-682.
468 Inagaki, S., Koiwai, A., Suzuki, N., Fukushima, Y., Kuroda, K., 1996. Synthesis of highly
469 ordered mesoporous materials, FSM-16, derived from kanemite. Bulletin of Chemical
470 Society of Japan. 69, 1449-1457.
471 Jaynes, W.F., Boyd, S.A., 1991. Clay mineral type and organic-compound sorption by
472 hexadecyltrimethlyammonium-exchanged clays. Soil Science Society of American
473 Journal 55, 43-48.
474 Kimura, T., Itoh, D., Okazaki, N., Kaneda, M., Sakamoto, Y., Terasaki, O., Sugahara, Y.,
475 Kuroda, K., 2000. Lamellar hexadecyltrimethylammonium silicates derived from
476 kanemite. Langmuir 16, 7624-7628.
477 Kimura, T., Kuroda, K., 2009. Ordered mesoporous silica derived from layered Silicates.
478 Advanced Functional Materials 19, 511-527.
479 Kuroda, K., 1996. Silica-Based Mesoporous Molecular Sieves Derived from a Layered
480 Polysilicate Kanemite-A Review. Journal of Porous Material 3, 107-114.
481 Lagaly, G., 1979. Crystalline silicic acids and their interface reactions. Advanced Colloid
482 Interface Science 11, 105-148.
483 Liebau, F. (Ed.), 1985. Structural Chemistry of Silicates; Springer-Verlag: Berlin,
484 Heidelberg, Germany.

485 Lippman, E., Maegi, M., Samoson, A., Engelhardt, G., Grimmer, A.R., 1980. Structural
486 studies of silicates by solid-state high-resolution Si-29 NMR. Journal of American
487 Chemical Society 102, 4889-4893.
488 Massiot, D., Fayon, F., Capron, M., King, I., Le Calvé, S., Alonso, B., Durand, J.O., Bujoli,
489 B., Gan, Z., Hoaston, G., 2002. Modelling one- and two-dimensional solid-state NMR
490 spectra. Magnetic Resonance Chemistry 40, 70-76.
491 Ogawa, M., Kuroda, K., 1995. Photofunctions of intercalation compounds. Chemical
492 Review 95, 399-438.
493 Ogawa, M., Kuroda, K., 1997. Preparation of inorganic-organic nanocomposites through
494 intercalation of organoamonium ions into layered silicates. Bulletin of Chemical
495 Society of Japan 70, 2593-2618.
496 Önal, M., Sarikaya, Y., 2008. Thermal analysis of some organoclays. Journal of Thermal
497 Analysis and Calorimetry, 91, 261-265.
498 Osman, M. A., Ploetze, M., Suter, U.W., 2003. Surface treatment of clay minerals-thermal
499 stability, basal-plane spacing and surface coverage. Journal Material Chemistry 13,
500 2359-2366.
501 Osman, M. A., Seyfang, G., Suter, U. W., 2000. Two-dimensional melting of alkane
502 monolayers ionically bonded to mica. Journal of Physical Chemistry B 104, 4433-4439.
503 Osman, M. A., Suter, U. W., 2002. Surface treatment of calcite with fatty acids: Structure
504 and properties of the organic monolayer. Chemistry Materials 14, 4408-4415.
505 Pazos, M.C., Castro, M.A., Orta, M.M., Pavon, E., Rios, J.S.V., Alba, M.D., 2012.
506 Synthetic high-charge organomica: Effect of the layer charge and alkyl chain length on
507 the structure of the adsorbed surfactants. Langmuir 28, 7325-7332.

508 Pinnavaia, T.J., Lan, T., Wang, Z., Shi, H., Kaviratna, P.D., 1996. Clay-reinforced epoxy
509 nanocomposites: Synthesis, properties, and mechanism of formation. Nanotechnology:
510 Molecularly Designed Materials. ACS Symposium Series 622, 250-261.
511 Rafailovich, M., Si, M., Goldman, M. (Eds.), 2003. PCT Int. Appl. (The Research
512 Foundation of State University of New York, USA), Wo, p. 34.
513 Sand, I.D., Piner, R.L., Gilmer, J.W., Owens, J.T. (Eds.), 2003. U.S., Eastman Chemical
514 Company, USA, p. 8.
515 Sutton, P.A. (Eds.), 2000. Proceedings of the 78th Annual Meeting Technical Program of
516 the FSCT p. 637.
517 Tamura, H., Mochizuki, D., Kimura, T., Kuroda, K. 2007. Formation of mesoporous silica
518 from a layered polysilicate makatite. Chemical Letter, 36, 444-445.
519 Taylor, R.S., Davies, M.E., Williams, J., 1992. PCT Int. Appl., Laporte Industries Ltd., UK,
520 Wo, p. 16.
521 Vortmann, S., Rius, J., Marler, B., Gies, H., 1999. Structure solution from powder data of
522 the hydrous layer silicate kanemite, a precursor of the industrial ion exchanger SKS-6.
523 European Journal of Mineralogy 11, 125-134.
524 Wang, L.Q., Liu, J., Exarhos, G.J., Brunker, B.C., 1996. Investigation of the structure and
525 dynamics of surfactant molecules in mesophase silicates using solid-state ^{13}C NMR.
526 Langmuir 12, 2663-2669.
527 Wang, L.Q., Liu, J., Exarhos, G.J., Flanigan, K.Y., Bordia, R. 2000. Conformation
528 heterogeneity and mobility of surfactant molecules in intercalated clay minerals studied
529 by solid-state NMR. Journal of Physical Chemistry B 104, 2810-2816.
530 Weiss, A., 1963. Organische derivate der glimmerartigen schichtslicate. Angewandte
531 Chemie, 75, 113-122

532 Xi, Y., Ding, Z., He, H., Frost, R.L., 2005. Infrared spectroscopy of organocays synthesized
533 with the surfactant octadecyltrimethylamonium bromide. Spectrochimica Acta Part A.
534 61, 515-525.
535 Xie, W., Gao, Z., Pan, W.P., Hunter, D., Singh, A., Vaia, R., 2001. Thermal degradation
536 chemistry of alkyl quaternary ammonium montmorillonite. Chemistry of Materials, 13,
537 2979-2990.
538 Yanagisawa, T., Shimizu, T., Kuroda, K.; Kato, C., 1990. The preparation of
539 alkyltrimethylammonium-kanemite complexes and their conversion to microporous
540 materials. Bulletin of Chemical Society of Japan 63, 988-992.
541 Yariv, S., 1996. Thermo-IR-spectroscopy analysis of the interactions between organic
542 pollutants and clay minerals. Thermochimica Acta 274, 1-35.
543 Yesinowski, J.P., Eckert, H., Rossman, G.R., 1988. Characterization of hydrous species in
544 minerals by high-speed H-1 MAS NMR. Journal of the American Chemical Society
545 110, 1367-1375.
546 Zhao, H., Vance, G.F., 1998. Sorption of trichloroethylene by organo-clays in the presence
547 of humic substance. Water Research 32, 3710-3716.

Table 1. Names of the ODTMA-Kanemites and synthesis conditions. Water and ODTMA content derived from TG analysis and Q^4 content calculated from ^{29}Si MAS NMR

					% w/w		
Product Name	ODTMA/ Si molar ratio	pH adjustment	T	t	Water[a]	ODTMA[b]	Q^4/Q^4+Q^3
Kanemite	--	--	--	--	23.58	5.05[g]	--
ODTMA-K-1[w,f]	0.18	No	70 ºC	3 days	22.85	17.65[d]	0.27
ODTMA-K-2[w,c]	0.18	No	70 ºC	3 days	23.49	19.08[d]	0.18
ODTMA-K-3[f]	0.18	No	70 ºC	3 days	14.01	34.22[d]	0.27
ODTMA-K-4[c]	0.18	No	70 ºC	3 days	19.54	30.30[d]	0.27
ODTMA-K-5[w,f]	0.18	No	70 ºC	2 days	18.70	17.34[d]	0.15
ODTMA-K-6[w,f]	0.18	No	70 ºC	7 days	19.19	29.34[d]	0.26
ODTMA-K-7[w,f]	0.18	No	90 ºC	2 days	19.25	31.22[d]	0.38
ODTMA-K-8[w,f]	0.18	No	90 ºC	3 days	17.93	21.98[d]	0.41
ODTMA-K-9[w,f]	0.18	No	90 ºC	7 days	15.59	29.66[d]	0.43
ODTMA-K-10[w,f]	0.18	HCl	90 ºC	3 days	6.73	36.69[d]	0.42
ODTMA-K-11[w,f]	0.18	HF	90 ºC	3 days	7.69	33.55[d]	0.48
ODTMA-K-12[w,f]	0.92	No	70 ºC	3 days	20.44	35.65[e]	0.41
ODTMA-K-13[w,f]	1.84	No	70 ºC	3 days	16.09	43.18[e]	0.52

(w) washed
(f) separation of ODTMA by filtration
(c) separation of ODTMA by centrifugation
(a) weight loss in the temperature range of 25 ºC-200 ºC
(b) weight loss in the temperature range of 200 ºC-550 ºC and corrected to dehydrated samples
(d) CEC of kanemite ($ODTMA_{0.36}Na_{0.64}[Si_2O_4(OH)]$ structural unit, based on the initial ODTMA/Si molar ratio) corresponds to a weight loss of ODTMA of 42.54%.
(e) CEC of kanemite ($ODTMA[Si_2O_4(OH)]$ structural unit) corresponds to a weight loss of ODTMA of 69.49%.
(g) weight loss due to dehydroxylation

FIGURE CAPTIONS

Fig. 1. XRD patterns (left) and ^{13}C MAS NMR spectra (right) of ODTMA-Kanemite synthesized at different ODTMA removal method (see Table 1). K=*020* reflection of Na-kanemite; t= all-*trans* configuration; and; g= dynamic average between the *gauche* and *trans* configurations.

Fig. 2. XRD patterns (left) and ^{13}C MAS NMR spectra (right) of ODTMA-Kanemite synthesized at different temperature and time of stirring (see Table 1). K=*020* reflection of Na-kanemite; t= all-*trans* configuration; and; g= dynamic average between the *gauche* and *trans* configurations.

Fig. 3. XRD patterns (left) and ^{13}C MAS NMR spectra (right) of ODTMA-Kanemite synthesized at different dispersion pH (see Table 1). K=*020* reflection of Na-kanemite; t= all-*trans* configuration; and; g= dynamic average between the *gauche* and *trans* configurations.

Fig. 4. XRD patterns (left) and ^{13}C MAS NMR spectra (right) of ODTMA-Kanemite synthesized at different ODTMA/Si molar ratios (see Table 1). K=*020* reflection of Na-kanemite; t= all-*trans* configuration; and; g= dynamic average between the *gauche* and *trans* configurations.

Fig. 5. ^{29}Si MAS NMR spectra (left) and IR/FT spectra (right) of ODTMA-Kanemite synthesized at different ODTMA removal method (see Table 1). *=IR bands of ODTMA, and, += IR band of five-member ring.

Fig. 6. ^{29}Si MAS NMR spectra (left) and IR/FT spectra (right) of ODTMA-Kanemite synthesized at different temperature and time of stirring (see Table 1). *=IR bands of ODTMA, and, += IR band of five-member ring.

Fig. 7. ^{29}Si MAS NMR spectra (left) and IR/FT spectra (right) of ODTMA-Kanemite synthesized at different dispersion pH (see Table 1). *=IR bands of ODTMA, and, += IR band of five-member ring.

Fig. 8. ^{29}Si MAS NMR spectra (left) and IR/FT spectra (right) of ODTMA-Kanemite synthesized at different ODTMA/Si molar ratios (see Table 1). *=IR bands of ODTMA, and, += IR band of five-member ring.

Figure 1

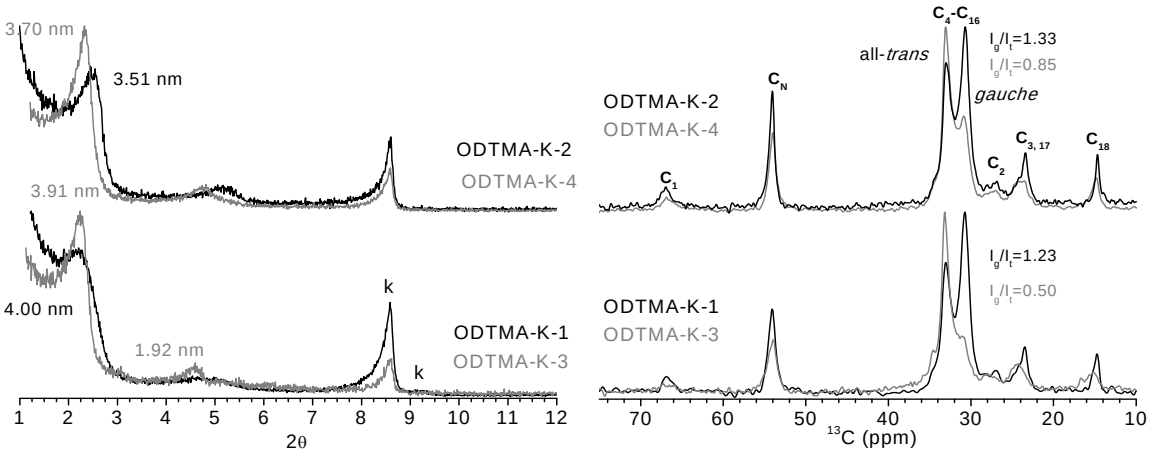
3.70 nm
3.51 nm
ODTMA-K-2
ODTMA-K-4
3.91 nm
4.00 nm
k
ODTMA-K-1
ODTMA-K-3
1.92 nm
k
1 2 3 4 5 6 7 8 9 10 11 12
2θ
C4-C16
all-trans
Ig/It=1.33
Ig/It=0.85
gauche
CN
ODTMA-K-2
ODTMA-K-4
C1
C2
C3, 17
C18
Ig/It=1.23
Ig/It=0.50
ODTMA-K-1
ODTMA-K-3
70 60 50 40 30 20 10
13C (ppm)

Figure 2

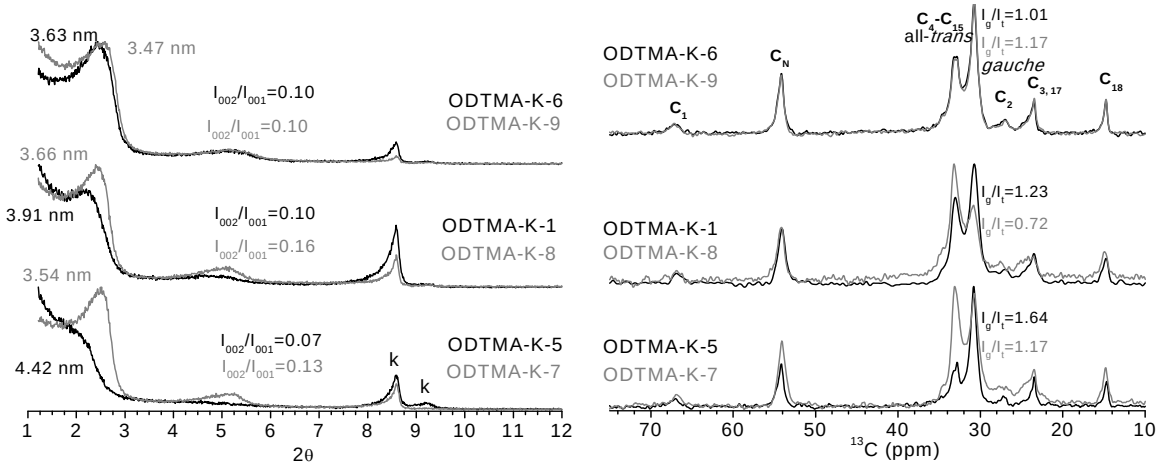
3.63 nm
3.47 nm
I002/I001=0.10
I002/I001=0.10
ODTMA-K-6
ODTMA-K-9
3.66 nm
3.91 nm
I002/I001=0.10
I002/I001=0.16
ODTMA-K-1
ODTMA-K-8
3.54 nm
4.42 nm
I002/I001=0.07
I002/I001=0.13
k
k
ODTMA-K-5
ODTMA-K-7
1 2 3 4 5 6 7 8 9 10 11 12
2θ
ODTMA-K-6
ODTMA-K-9
CN
C1
C4-C15
all-trans
Ig/It=1.01
Ig/It=1.17
gauche
C2
C3, 17
C18
ODTMA-K-1
ODTMA-K-8
Ig/It=1.23
Ig/It=0.72
ODTMA-K-5
ODTMA-K-7
Ig/It=1.64
Ig/It=1.17
70 60 50 40 30 20 10
13C (ppm)

Figure 3

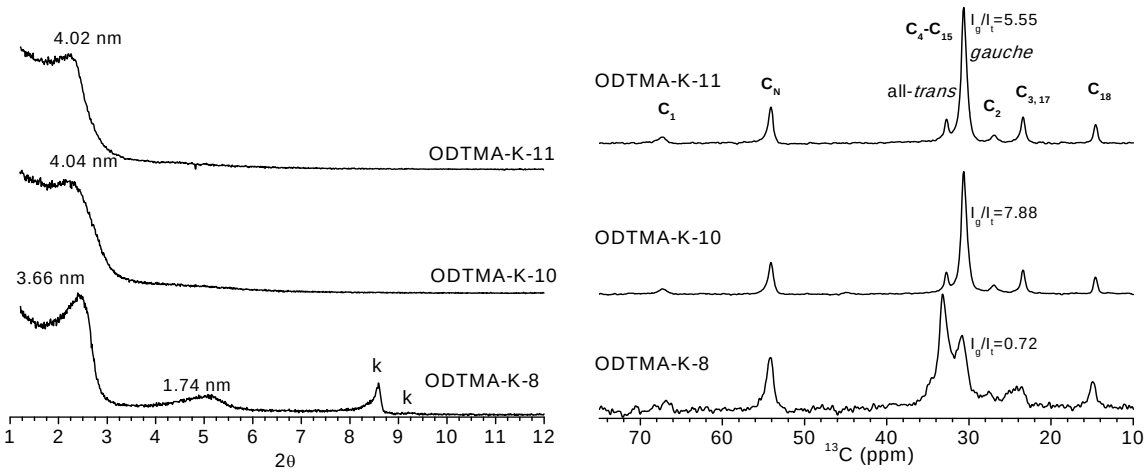
4.02 nm
ODTMA-K-11
4.04 nm
ODTMA-K-10
3.66 nm
1.74 nm
k
k
ODTMA-K-8
1 2 3 4 5 6 7 8 9 10 11 12
2θ
ODTMA-K-11
C1
CN
C4-C15
Ig/It=5.55
gauche
all-trans
C2
C3, 17
C18
ODTMA-K-10
Ig/It=7.88
ODTMA-K-8
Ig/It=0.72
70 60 50 40 30 20 10
13C (ppm)

Figure 4

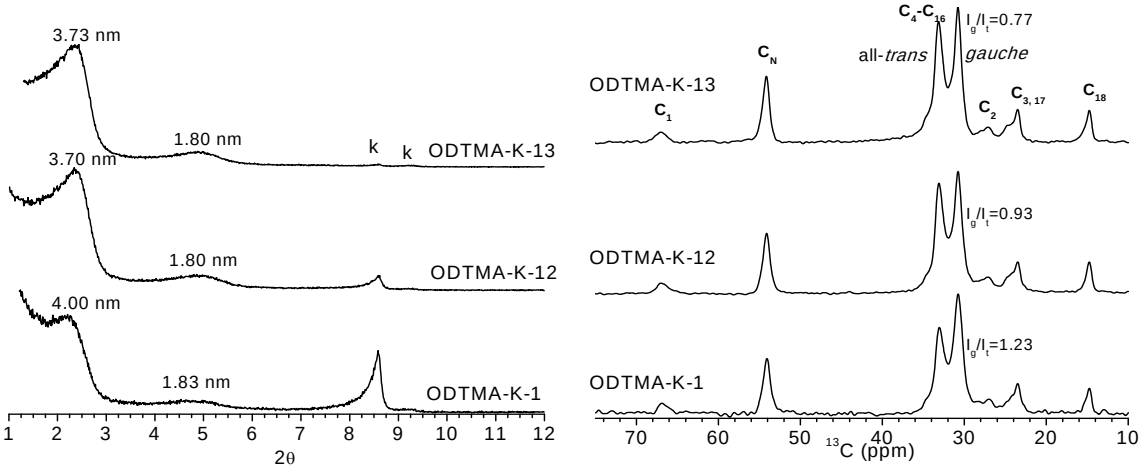
3.73 nm
1.80 nm
k
k
ODTMA-K-13
3.70 nm
1.80 nm
ODTMA-K-12
4.00 nm
1.83 nm
ODTMA-K-1
1 2 3 4 5 6 7 8 9 10 11 12
2θ
C4-C16
Ig/It=0.77
CN
all-trans
gauche
ODTMA-K-13
C1
C2
C3, 17
C18
Ig/It=0.93
ODTMA-K-12
Ig/It=1.23
ODTMA-K-1
70 60 50 40 30 20 10
13C (ppm)

Figure 5

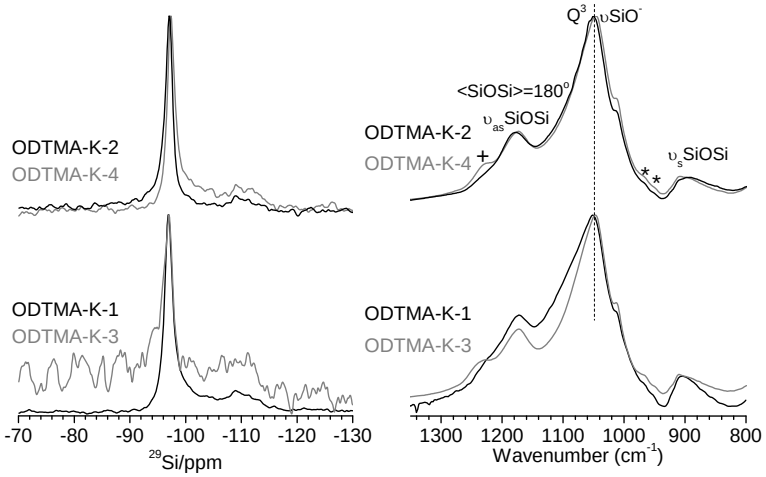
ODTMA-K-2
ODTMA-K-4
ODTMA-K-1
ODTMA-K-3
-70 -80 -90 -100 -110 -120 -130
29Si/ppm
Q3 υSiO-
<SiOSi>=180°
υas SiOSi
υs SiOSi
+
*
1300 1200 1100 1000 900 800
Wavenumber (cm-1)

Figure 6

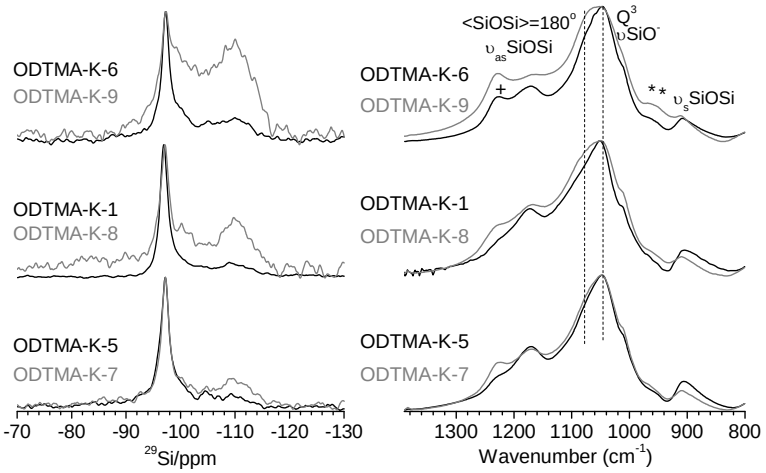
ODTMA-K-6
ODTMA-K-9
ODTMA-K-1
ODTMA-K-8
ODTMA-K-5
ODTMA-K-7
-70 -80 -90 -100 -110 -120 -130
29Si/ppm
<SiOSi>=180°
υas SiOSi
Q3
υSiO-
+
** υs SiOSi
1300 1200 1100 1000 900 800
Wavenumber (cm-1)

Figure 7

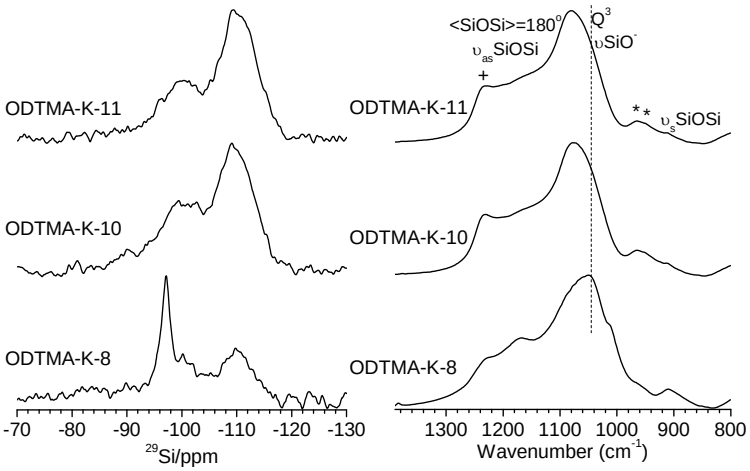
ODTMA-K-11
ODTMA-K-10
ODTMA-K-8
-70 -80 -90 -100 -110 -120 -130
29Si/ppm
<SiOSi>=180°
Q3
υSiO-
υasSiOSi
+
**
υsSiOSi
ODTMA-K-11
ODTMA-K-10
ODTMA-K-8
1300 1200 1100 1000 900 800
Wavenumber (cm-1)

Figure 8

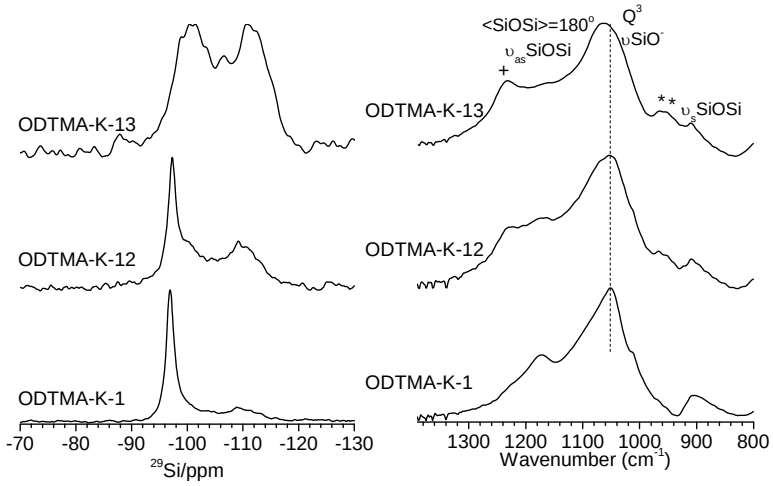
ODTMA-K-13
ODTMA-K-12
ODTMA-K-1
-70 -80 -90 -100 -110 -120 -130
29Si/ppm
<SiOSi>=180°
Q3
υSiO-
υas SiOSi
+
** υs SiOSi
ODTMA-K-13
ODTMA-K-12
ODTMA-K-1
1300 1200 1100 1000 900 800
Wavenumber (cm-1)